Sample	Depth	$^{210}Pb_{xs}$ (mBq/g)	^{137}Cs (mBq/g)
Core 1			
	0.5	101 ± 31	-2 ± 3
	10.5	131 ± 12	3 ± 1
	21.5	88 ± 5	3 ± 0
	30.5	58 ± 11	4 ± 1
Core 2			
	1.5	90 ± 6	3 ± 0
	10.5	80 ± 7	2 ± 1
	20.5	58 ± 4	3 ± 0
	35.5	32 ± 4	1 ± 0
Core 3			
	0.5	127 ± 15	0 ± 1
	10.5	110 ± 15	1 ± 1
	20.5	68 ± 14	1 ± 1

Table 1. $^{210}Pb_{xs}$ and ^{137}Cs activities in sediments.

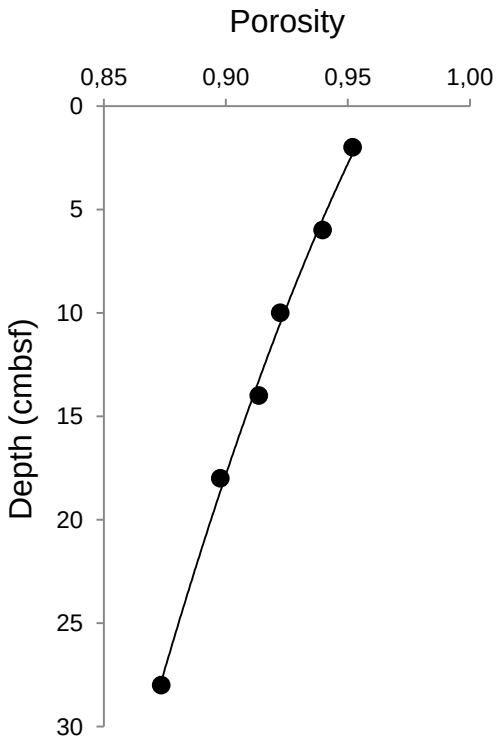

Fig 1. Depth profile of porosity in sediments.

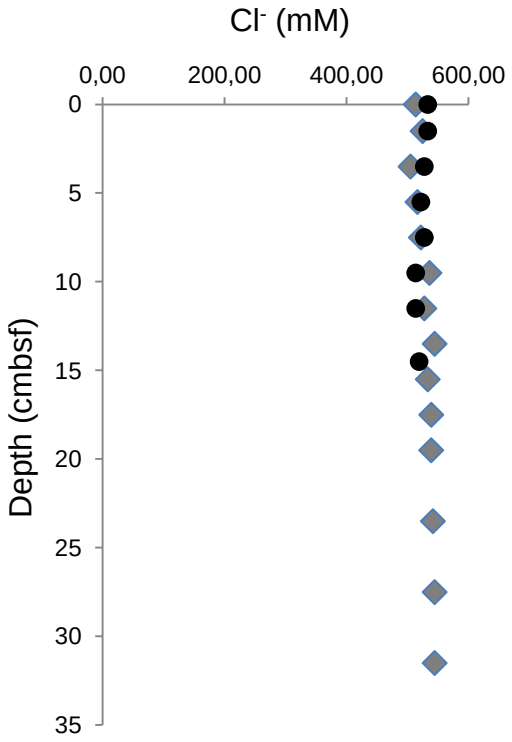

Fig 2. Depth profiles of chloride in sediments.

1. Steady State model

In the steady state model, we first fit the sulfate profiles shallower than 20 cm from Core 1&2 with a 2-order polynomial trend. Sulfate concentration below 20 cm was assumed to be constant (0.28 mM). The $\delta^{34}S$ of sulfate was fitted in the same fashion. After deriving $^{34}S/^{32}S$ ratios from the fitted trend of $\delta^{34}S$ record (assuming the Canyon Diablo Troilite standard has the ^{34}S to ^{32}S ratio of 0.0450045), we calculated concentrations of ^{32}S total sulfate concentration. We set 16 grids for the 40-cm sediment column. For each grid, we calculated the input flux (with Fick's first law) for both ^{34}S and ^{32}S of sulfate from the grid above the target grid and output fluxes towards the grid below. The net SRR at each grid is the difference between the input and out fluxes. Porosity was assumed to be 0.9 and diffusion coefficient for sulfate as 0.0337 m^2/yr (Boudreau, 1997).

After estimating the net SRR for ^{32}S (i.e., sum of $^{32}R_{AOM}$ and $^{32}R_{OSR}$), we assumed the rate constants for OSR and AOM-SR differently in the three modes we tested. In the "constant-k" mode, we assumed all SR can be attributed to OSR until 17.5 cmbsf (i.e., no AOM-SR until that level). AOM-SR only happens in the grid of 20cm, where most sulfate is consumed. Rate constants for OSR with respect to ^{32}S were assumed to be "1" (a unitless scaling parameter). AOM-SR rates ($^{32}R_{AOM}$) for ^{32}S were calculated from

the difference of net SRR and OSR rates; rate constants ($^{32}k_{AOM}$) were estimated following the expression:

$$^{32}k_{AOM} = {}^{32}R_{AOM} / {}^{32}SO_4 \quad (S1)$$

which is 0 m/yr until 17.5 cm and 1.35 m/yr at 20 cm. The fractionations (ε) of OSR and AOM-SR were estimated in a rate-dependent fashion (Dale et al., 2009):

$$\varepsilon_i = \varepsilon_{max} - m_{SR} * R_i \quad (S2)$$

Where i = AOM or OSR and ε_{max} is the theoretical maximum fractionation, R is the net rate of OSR or AOM-SR (i.e., $^{32}R + {}^{34}R$) and m_{SR} determines the variability of fractionation with rates. We used 78‰ for ε_{max} and 1.5 yr/mM for m_{SR} following the suggestions from Dale et al. (2009) and Farquhar et al. (2003). The rate constants, $^{34}k_{AOM}$ and $^{34}k_{OSR}$, can then be estimated following:

$$^{32}k_i / {}^{34}k_i = \alpha_I \quad (S3)$$

$$\alpha_i = 1+\varepsilon_i/1000 \quad (S4)$$

where i = AOM or OSR and α is the fractionation factors for particular pathways. Once we estimated $^{34}R_{AOM}$ and $^{34}R_{OSR}$ following the similar fashion of Eq.(S1), we can calculated the concentration of $^{34}SO_4$ as based on these rates and fluxes from grid above and below. $\delta^{34}S$ was then estimated from the concentration of $^{32}SO_4$ and $^{34}SO_4$, and compared with the observed values.

For the “variable-k” mode, all the calculation is the same as above except that we assumed $^{32}k_{OSR}$ decreases by 0.05 for each grid deeper “. $^{32}k_{OSR}$ decreases follow the exact fashion with sediment age as proposed by Middelburg (1989) in the “Middelburg mode”. The age of the sediment was estimated from the sedimentation rate (7.6 m/yr).

The major uncertainties of this calculation lay within the values assigned for Eq.(S2) and the age dependency of k_{OSR}. It is therefore more important to pay attention to the structure of the profiles than the absolute values. All models can reproduce the structure of our measured $\delta^{34}S$ profiles.

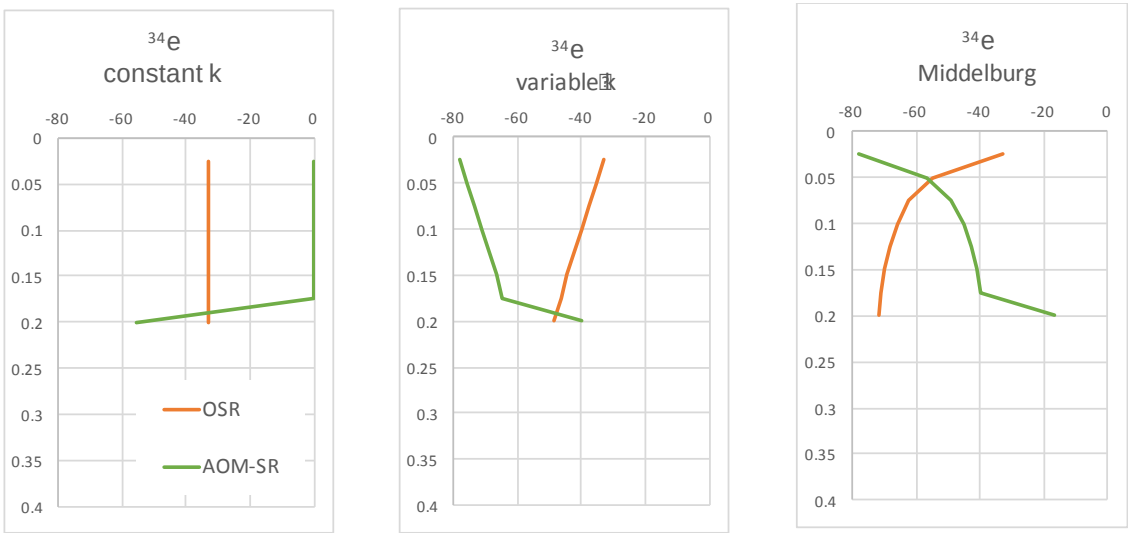

Fig 3. Fractionations applied to AOM-SR and OSR.

2. Non-steady state model

For our non-steady state model, we coupled CrunchFlow (Steefel, 2009) with a customized MATLAB code to simulate reactions, diffusion, and sediment burial. This modeling strategy has been successfully applied by Hong et al. (2016). More details were provided in the aforementioned paper. In this model, we simulation the fluid evolution for a 20-cm sediment column with 200 grids (0.1 cm thick for each grid) over a time course of 25 years. CrunchFlow evaluated diffusion and reactions for each 2.5-year time slice; our MATLAB code then simulate the burial of both pore fluid and sediments for this 2.5 years. We assumed both liquid and solid phases were buried for a same rate; in other words, compactional fluid advection is excluded in the current model. We included 8 primary chemical species (sulfate, methane, hydrogen sulfide, ammonium, phosphate, chloride, bicarbonate, and sodium) and another 8 secondary chemical species (CO_2, CO_3^{2-}, H_3PO_4, $H_2PO_4^-$,PO_4^{3-}, H_2S, and S^{2-}) to account for effects from ionic strength, charge balance, and pH in the pore fluid. See Hong et al. (2014) for the detail reactions of the secondary species. The secondary species responses not only to the primary reactions we assigned (AOM-SR and OSR in this case) but also any redistribution of primary species due to diffusion and burial. OSR was formulated as *Monod-type* rate expression with one *Monod* term:

$$ROSR = A_m k_m \exp[\frac{-Ea}{RT}]\prod a_i^n[1-\frac{Q}{K_{eq}}] \quad \text{(S5)}$$

$$k_m = k_{\max}^{OSR}\left(\frac{C_{SO4}}{C_{SO4}+K_{half}}\right) \quad \text{(S6)}$$

where A_m (=1) and k_m are the surface area and kinetic constant. *Ea*, *R*, and *T* are the activation energy, ideal gas constant, and temperature. Πa_i^n is the activity product of solutes in the reaction with their stoichiometry (*n*) as exponents. $\frac{Q}{K_{eq}}$ determines the direction of reaction where *Q* is the ion activity product and K_{eq} is the equilibrium constant. As OSR is a kinetic-driven reaction, we arbitrarily assigned a K_{eq} to ensure the reaction always in a forward direction. $k_{\max}^{POCSR}$ is the theoretical maximum rate that was assigned based on our assumption of organic matter reactivity (Table S2). K_{half} is the half saturation constant (=100 μM; Wegener and Boetius, 2009), and C_{SO4} is the concentration of sulfate.

AOM-SR was formulated as *Monod-type* reactions with two *Monod* terms:

$$R_{AOM} = k_{\max}^{AOM}\left(\frac{C_{SO_4}}{C_{SO_4}+K_{half-SO_4}}\right)\left(\frac{C_{CH_4}}{C_{CH_4}+K_{half-CH_4}}\right)\left(1-\frac{Q}{K_{eq}}\right) \quad \text{(S7)}$$

where *C* is the concentration of electron donors or acceptors and *Q* is the ion activity product.

$K_{half-SO_4}$ and $K_{half-CH_4}$ were set to be 500 μM (Wegener and Boetius, 2009) and 5 mM (Nauhaus et al., 2002; Vavilin, 2012), respectively. $k_{\max}^{AOM}$, was obtained from fitting curves to our data.

The four scenarios we assigned in this work are different with respect to the reactivity of organic matter, modes of sedimentation, initial conditions, and the time scale focused. Table S2 listed the different setup for the four scenarios.

	Scenario 1	**Scenario 2**	**Scenario 3**	**Scenario 4**
Top boundary condition	Topmost measured values	Topmost measured values	Topmost measured values	Topmost measured values
Bottom boundary condition	No flux boundary for sulfate	No flux boundary for sulfate	No flux boundary for sulfate	No flux boundary for sulfate
Initial condition	Same as top boundary	Same as top boundary	The results from scenario 2	The results from scenario 2
Temporal scale (yr)	25	25	12.5	0.25
Depth scale	20	20	20	20

(cm)				
Theoretical maximum OSR rate (mol.kg (H_2O) $^{-1}$.yr^{-1})	10^{-6}	$10^{-6.5}$	10^{-6} for the first 10 cm and 0 below	$10^{-4.9}$ for the first 5 cm and 0 below
Sedimentation rate	Constant sedimentation	Constant sedimentation	Constant sedimentation	No sedimentation except for the instantaneous input of the first 5 cm layer

Table 2. Different conditions assigned for the four scenarios.

References

Boudreau, B.P., 1997. Diagenetic models and their implementation: modelling transport and reactions in aquatic sediments. Springer.

Dale, A.W., Brüchert, V., Alperin, M., Regnier, P., 2009. An integrated sulfur isotope model for Namibian shelf sediments. Geochim. Cosmochim. Acta 73, 1924–1944. doi:10.1016/j.gca.2008.12.015

Farquhar, J., Johnston, D.T., Wing, B.A., Habicht, K.S., Canfield, D.E., Airieau, S., Thiemens, M.H., 2003. Multiple sulphur isotopic interpretations of biosynthetic pathways: implications for biological signatures in the sulphur isotope record. Geobiology 1, 27–36. doi:10.1046/j.1472-4669.2003.00007.x

Hong, W.-L., Sauer, S., Panieri, G., Ambrose, W.G., James, R.H., Plaza-Faverola, A., Schneider, A., 2016. Removal of methane through hydrological, microbial, and geochemical processes in the shallow sediments of pockmarks along eastern Vestnesa Ridge (Svalbard). Limnol. Oceanogr. n/a-n/a. doi:10.1002/lno.10299

Hong, W.-L., Torres, M.E., Kim, J.-H., Choi, J., Bahk, J.-J., 2014. Towards quantifying the reaction network around the sulfate–methane-transition-zone in the Ulleung Basin, East Sea, with a kinetic modeling approach. Geochim. Cosmochim. Acta 140, 127–141. doi:10.1016/j.gca.2014.05.032

Middelburg, J.J., 1989. A simple rate model for organic matter decomposition in marine sediments. Geochim. Cosmochim. Acta 53, 1577–1581. doi:10.1016/0016-7037(89)90239-1

Nauhaus, K., Boetius, A., Krüger, M., Widdel, F., 2002. In vitro demonstration of anaerobic oxidation of methane coupled to sulphate reduction in sediment from a marine gas hydrate area. Environ. Microbiol. 4, 296–305. doi:10.1046/j.1462-2920.2002.00299.x

Steefel, C.I., 2009. CrunchFlow. Softw. Model. Multicomponent React. Flow Transp. User's Man. Lawrence Berkeley Natl. Lab. Berkeley USA.

Vavilin, V.A., 2012. Estimating changes of isotopic fractionation based on chemical kinetics and microbial dynamics during anaerobic methane oxidation: apparent zero- and first-order kinetics at high and low initial methane concentrations. Antonie Van Leeuwenhoek 103, 375–383. doi:10.1007/s10482-012-9818-8

Wegener, G., Boetius, A., 2009. An experimental study on short-term changes in the anaerobic oxidation of methane in response to varying methane and sulfate fluxes. Biogeosciences 6, 867–876. doi:10.5194/bg-6-867-2009